Calculation of Static (Hyper)polarizabilities for π-Conjugated Donor/Acceptor Molecules and Block Copolymers by the Elongation Finite-Field Method

S. Ohnishi,[†] F. L. Gu,[‡] K. Naka,[§] A. Imamura,[||] B. Kirtman,*[,⊥] and Y. Aoki[†,‡]

Department of Molecular and Material Sciences, Interdisciplinary Graduate School of Engineering Sciences, Kyushu University, 6-1 Kasuga-Park, Fukuoka, 816-8580, Japan, Group, PRESTO, Japan Science and Technology Agency (JST), Kawaguchi, Center Building, Honcho 4-1-8, Kawaguchi, Saitama, 332-0012, Japan, Department of Chemistry, Graduate School of Science, Hiroshima University, Kagamiyama 1-3-1, Higashi-Hiroshima 739-8526, Japan, Department of Mathematics, Faculty of Engineering, Hiroshima Kokusai Gakuin University, Nakano 6-20-1, Aki-ku, Hiroshima-city, 739-0321, Japan, and Department of Chemistry and Biochemistry, University of California, Santa Barbara, California 93106

Received: May 14, 2004; In Final Form: July 17, 2004

The elongation finite-field (elongation-FF) method is applied to calculate static (hyper)polarizabilities of π-conjugated chains, with donor and/or acceptor substituents, as well as a heterol block copolymer. Substituent effects on the linear polarizability (α) and second hyperpolarizability (γ) are modest, but a large first hyperpolarizability (β) can be induced. The dependence of β on chain length is rationalized on the basis of quasi-symmetry and donor/acceptor strength. Our copolymer consists of alternating blocks containing pyrrole rings and silole rings, which generates a quantum well. Copolymerization induces a fairly small β that oscillates in sign from block to block. The effect on α and γ is to enhance the contribution of the pyrrole blocks and diminish, by a larger amount, the contribution of the silole blocks.

I. Introduction

In recent years, nonlinear optical (NLO) materials have drawn increasing attention due to their potential utilization in optical and electro-optical devices. Organic π-conjugated compounds are of particular interest since their properties can be readily tailored by chemical modification. In this regard, molecular design can be helpful to experimentalists who wish to synthesize NLO molecules, polymers, and other materials with desired properties.

From a theoretical point of view, the NLO properties of periodic polymers can be determined by several approaches. One of these is a finite cluster treatment in which the NLO properties of an infinitely extended polymer are determined by extrapolating values obtained for finite oligomers.[1−3] Another approach is based on crystal orbital techniques,[4−6] wherein periodic boundary conditions (PBCs) are imposed to take advantage of translational symmetry. Recently, Kirtman et al.[7] have shown how to apply PBCs in the presence of electric fields using time-dependent Hartree−Fock perturbation theory. Both static[8−10] and dynamic[11,12] (hyper)polarizabilities have been calculated by the latter method. However, in the first approach, convergence with increasing chain length is slow for π-conjugated systems, while in the second, application is currently restricted to polymers containing small unit cells. This restricts utilization for block copolymers or aperiodic polymers.

In the early 1990s, an elongation method for calculating electronic states of large systems at the Hartree−Fock level was developed by Imamura et al.[13,14] This approach, which can be applied to aperiodic as well as periodic systems, is a procedure for sequentially adding arbitrary fragments to a starting cluster. Recently, the elongation procedure was extended to include a perturbing static finite electric field (i.e., the elongation-FF method)[15] and used to determine static (hyper)polarizabilities of long-chain oligomers. The primary purpose of the current paper is to demonstrate the applicability of this method to long-chain donor (D) and/or acceptor (A) molecules with various substitution patterns and to block copolymers as well. Thus, we examine terminal donor and/or acceptor substituents on polyacetylene (PA) and poly(paraphenylene) (PPP) chains, more general substitution patterns on poly(*para*-phenylene-ethynylene) (PPE) chains, and a π-conjugated block copolymer of pyrrole and silole containing a quantum well. Since our intent is primarily to provide a proof of the method, we have contented ourselves with employing the PM3 semiempirical Hamiltonian in these calculations.

In section II, the basic ideas and important computational aspects of the elongation-FF method are reviewed. Then, in section III we compare the results of elongation-FF to conventional calculations for a set of medium-length chains before going on to consider the extended chain length dependence. After that, the effect of varying the type and location of substituents is examined, and finally, we study the block copolymer with a quantum well that was mentioned above. This paper concludes with a summary of our major conclusions and future plans.

II. Method

Details of the Hartree−Fock elongation method and its application to a system perturbed by a uniform static electric field have been described in previous papers.[13−15] In this section, we present a brief overview. First, the canonical molecular orbitals (CMOs) of an oligomer containing several monomer units (the starting cluster) are obtained by solving the canonical

[†] Kyushu University.
[‡] Japan Science and Technology Agency (JST).
[§] Hiroshima University.
[||] Hiroshima Kokusai Gakuin University.
[⊥] University of California.

10.1021/jp047935c CCC: $27.50
Published on Web 09/08/2004

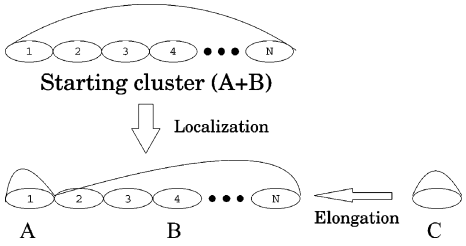

Figure 1. Schematic outline of elongation procedure.

$$\begin{array}{|ccccc|c} F^{OCC}(A,A)-\varepsilon I & 0 & F^{OCC}(A,B) & 0 & \sim 0 & \\ 0 & F^{VAC}(A,A)-\varepsilon I & 0 & F^{VAC}(A,B) & \sim 0 & \\ F^{OCC}(B,A) & 0 & F^{OCC}(B,B)-\varepsilon I & 0 & F^{OCC}(B,C) & = 0 \\ 0 & F^{VAC}(B,A) & 0 & F^{VAC}(B,B)-\varepsilon I & F^{VAC}(B,C) & \\ \sim 0 & \sim 0 & F^{OCC}(C,B) & F^{VAC}(C,B) & F^{OCC}(C)-\varepsilon I & \end{array}$$

Figure 2. Factorization of the Fock matrix. Only the section outlined by dashed lines is included in the elongation step.

Hartree−Fock (HF) equation. Next, as shown in Figure 1, the occupied and vacant CMOs are separately localized by unitary transformation either to region A or region B. Region A, which will be frozen, is at the opposite end of the chain from the attacking monomer (region C). This leaves region B as the active region that interacts with the attacking monomer. Details of the localization procedure have been described in ref 13.

The number of unit cells in the active region must be large enough to essentially isolate region A from the attacking monomer. Assuming that is so, then the orbitals on fragment C are allowed to interact only with localized molecular orbitals (LMOs) in region B. The interactions between regions A and B are minimized in the localization procedure. In preparation for elongation step, it is necessary to remove the terminal capping atom(s) (normally H atom(s)). This is done in two steps. First, the atomic orbital (AO) basis functions of the terminal atom(s) are removed from the LMOs. This creates linear dependencies among the LMOs of region B which, then, have to be removed. The linear dependencies correspond to the eigenvectors associated with zero eigenvalues that are obtained by diagonalizing the overlap matrix in the LMO representation.

Solution of the Hartree−Fock equation for the interactive region, that is, B + C, as indicated by the dashed lines in Figure 2, yields a set of occupied CMOs which, in combination with the occupied LMOs of region A, span the entire occupied space. The vacant molecular orbitals on B + C and A constitute the remainder of the full space. Finally, the occupied and vacant CMOs on B + C are separately localized in preparation for the next elongation step. It is critical that the size of the starting cluster is large enough so that there is no error buildup when the cluster is elongated.

A major advantage of the elongation method is that the dimension of the eigenvalue equation to be solved remains the same as the size of the cluster is increased. Although $F^{occ}(A,B)$ and $F^{vac}(A,B)$ are not included in the eigenvalue problem, their contribution to the energy cannot generally be neglected. $F^{vac}(A,B)$ contributes because the vacant orbitals of region B become partially occupied in the elongation step. We observe, however, that the effect of these coupling terms is readily calculated since the full density matrix and the full Fock matrix are available.[13]

A second major advantage is that monomer fragment C is variable from step to step so that one can readily construct block copolymers and donor−acceptor chains, as well as polymers with a random distribution of monomers. For the donor−acceptor species considered in this paper, the final monomer added to the growing chain contains a substituent group instead of a terminal hydrogen.

To get (hyper)polarizabilities for each elongation step, the above-described elongation method is implemented using the field-dependent Fock matrix,

$$F(\mathbf{E}) = H - \mathbf{E}\cdot\mathbf{r} + P(\mathbf{E})[2J - K] \tag{1}$$

In eq 1, **E** is the static electric field, H is the core Hamiltonian matrix, **r** is the vector sum of dipole moment matrices, $P(\mathbf{E})$ is the field-dependent density matrix, and J and K are coulomb and exchange supermatrices. The total energy in the presence of the electric field is expanded as

$$W(E) = W(0) - \mu_i E_i - \frac{1}{2}\alpha_{ij}E_iE_j - \frac{1}{6}\beta_{ijk}E_iE_jE_k - \frac{1}{24}\gamma_{ijkl}E_iE_jE_kE_l + \cdots \tag{2}$$

where, i, j, k, and l are Cartesian axes and the usual summation convention is used for repeated indices. When numerical differentiation is carried out, the molecular (hyper)polarizability tensors are evaluated as

$$\alpha_{ij} = \left(\frac{\partial^2 W(E)}{\partial E_i \partial E_j}\right)_{E=0}$$

$$\beta_{ijk} = \left(\frac{\partial^3 W(E)}{\partial E_i \partial E_j \partial E_k}\right)_{E=0}$$

$$\gamma_{ijkl} = \left(\frac{\partial^4 W(E)}{\partial E_i \partial E_j \partial E_k \partial E_l}\right)_{E=0} \tag{3}$$

For quasi-one-dimensional systems with push−pull substitutions at terminal positions on the polymer chain, the diagonal elements in the chain direction are the most important and we will focus on these elements although other systems where β is no longer longitudinally dominant will also be treated. Thus, we consider only the case where i, j, k, and l all refer to the polymer axis x. The present work is carried out at the PM3 semiempirical level where $W(E)$ is replaced by the heat of formation.

In the following calculations, we use the MP2/6-311G* geometry of PA as taken from ref 16. The geometries of PPP, PPE, polyheterol, and the substituted terminal units of PA and PPP derivatives were obtained at the HF/6-311G** level using Gaussian 98.[17]

III. Results and Discussion

A. Reliability of the Elongation-FF Method. In a previous paper (ref 15), we established the reliability of the elongation-FF method for (hyper)polarizabilities of H_2, H_2O, and PA chains. Since a major focus of this current work is on substituent effects, a preliminary test was carried out for PA chains substituted at one end by an NO_2 group, that is, $NO_2-(C_2H_2)_N-H$. A comparison of PM3 results calculated by the elongation-FF method with those obtained using the conventional finite-field procedure, implemented in the MOPAC program (MOPAC-FF), is reported in Table 1. The starting cluster for elongation-FF contained 20 units, which is the length found to be satisfactory for unsubstituted PA in ref 15, and the chain was elongated by one C_2H_2 unit at a time up to $N = 28$. For convenience, only the N even results are given. Although not

TABLE 1: Comparison between the Elongation-FF and MOPAC-FF Methods for $NO_2-(C_2H_2)_N-H$

N	MOPAC-FF	elongation-FF	relative error (%)
		α (au)	
22	3425.0	3425.0	0.00
24	3803.9	3804.0	0.00
26	4183.8	4183.9	0.00
28	4564.4	4564.4	0.00
		β (au)	
22	73 460	73 457	0.01
24	75 377	74 867	0.68
26	76 813	76 402	0.54
28	77 897	77 443	0.58
		γ (10^4 au)	
22	20 572	20 571	0.00
24	24 080	23 990	0.04
26	27 664	27 540	0.45
28	31 304	31 183	0.39

shown, the total energies for the two methods differ by less than 10^{-6} eV in every case. Consequently, the (hyper)-polarizabilities are quite similar. From Table 1, we see that the difference between the elongation-FF and MOPAC-FF values for α is always less than 0.01%, whereas the maximum difference for either β or γ is 0.68%. Although there is a small initial increase in the error upon increasing *N*, the important point is that the error does not accumulate as the chain is lengthened further. These results demonstrate the reliability of the elongation-FF method for an electron acceptor substituent.

B. Donor−Acceptor Substitution at Chain Ends of PA and PPP Oligomers. Based on the successful test in section A, we proceeded to examine oligomers of PA and PPP substituted at the chain end (in the para position for PPP) with various donor or acceptor groups, X (X = H, NH_2, NO_2, CN). The starting PA and PPP clusters for the elongation-FF calculations were taken as 20 units for the former and 10 for the latter (roughly equal path lengths in either case). The (hyper)polarizabilities of shorter chains were obtained using the conventional MOPAC-FF method. For longer chains, elongation-FF values were determined stepwise up to a length of 50 units for PA and 26 units for PPP.

Plots of α, β, and γ versus chain length (*N*) are shown for substituted PA chains in Figure 3a−c. The corresponding plots for PPP are given in Figure 4a−c. For sufficiently large *N*, the increment in the (hyper)polarizability due to addition of a monomer should not depend on X because the substituent effect is localized more or less to the chain end.[18,19] Consequently, as observed in Figures 3 and 4, the slope at large *N* is the same regardless of X. For β, that slope approaches zero since unsubstituted PA and PPP are both centrosymmetric. In the case of α and γ, the individual curves for each substituent are almost identical; the property values at large *N* differ by less than 2%. At small *N*, the deviation from a linear plot is modest for α, whereas γ deviates more significantly. Using the power law $\gamma \propto N^{\eta}$, we obtain $\eta = 3.9-4.7$ for $N \leq 16$ in the case of PA (X = H) while for $N \leq 7$ $\eta = 2.0-2.5$ in the case of PPP (X = H). This is in reasonable agreement with the corresponding values of 3.9−4.9 and 2.5−2.7 reported in ref 19.

In contrast with α and γ, the value of β grows much more rapidly in the short-chain regime than at large *N*. The onset of long-range behavior occurs at roughly $N = 15$ for substituted PA chains and at about $N = 7$ for substituted PPP chains. This is consistent with the difference in the π-conjugated path length along the backbone in the C_6H_4 unit cell as opposed to the C_2H_2 unit cell.

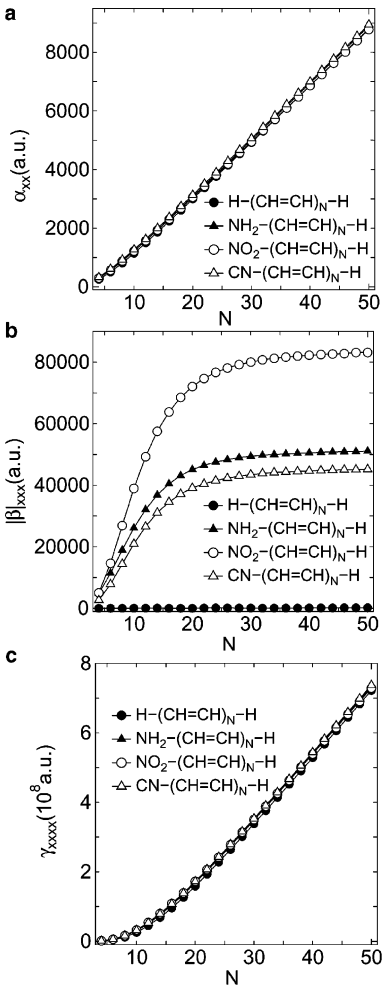

Figure 3. Dependence of (hyper)polarizabilities on the number of −(CH═CH)− units, *N*, for terminal D and/or A substitution at the opposite end of the growing PA chain: (a) α, (b) β, and (c) γ.

We then considered the same chains as above but with a donor or acceptor substituent at each end and in the para position for PPP. The treatment is unaltered except that the monomer added in the final elongation step now contains a terminal substituent. Our results for the longest chain are shown in Table 2. As before, we see that donor−acceptor substitution has a very modest effect on α and γ for both PA and PPP. On the other hand, the β values increase substantially as expected when one substituent is a donor and the other an acceptor. In PA with one substituent, NO_2 gives the largest β; double substitution with NO_2 and NH_2 increases that value by a factor of 1.61. For PPP, the analogous ratio is 2.15, although the absolute values of β are an order of magnitude smaller.

For the doubly substituted PA chain, with NO_2 on one end and NH_2 on the other, our result for β at $N = 50$ is 134×10^3 au. It is difficult to compare with previous ab initio calculations because only much smaller chains were considered in ref 20. However, an approximate extrapolation formula is given in that paper from which we obtain 132×10^3 au at the HF/6-31G level and 213×10^3 au at the MP2/6-31G level. Thus, PM3 gives reasonable values in this case.

Finally, we studied the effect of substituting at different positions on the terminal benzene rings of PPP. The various possibilities considered are shown in Figure 5, and the results for β are given in Table 3. α and γ have been omitted from the table because the values do not depend significantly on position as might have been anticipated from our previous results. β

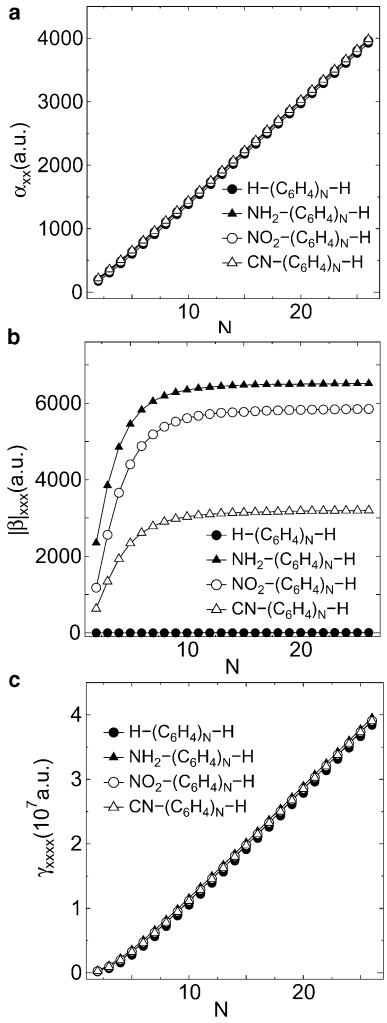

Figure 4. Dependence of (hyper)polarizabilities on the number of phenyl rings, *N*, for terminal D or A substitution at the opposite end of the growing PPP chain: (a) α, (b) β, and (c) γ.

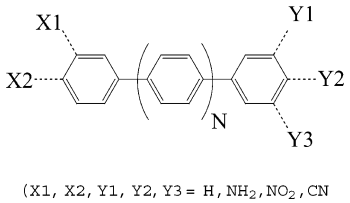

Figure 5. Various patterns considered for substitution at both ends of a PPP chain.

attains a maximum value when both members of the NH_2/NO_2 pair are in the para position. The next largest values occur when NO_2 is replaced by CN or moved to the meta position.

C. Substituent Effects along the Backbone of PPE Chains. The effect of various donor/acceptor substitutions on the phenyl rings along the backbone of PPE chains was investigated next. On the basis of a unit cell containing two phenyl-ethynyl groups, four different substitution patterns, exhibited in Figure 6 (models 1−4), were chosen for study along with the corresponding unsubstituted species (model 0). These models include substitution on either one or both phenyl rings. The starting clusters consisted of $N/2 = 4$ unit cells, or 8 phenyl-ethynyl groups, which were elongated one phenyl-ethynyl group at a time up to $N = 16$. This choice of starting cluster is consistent, in terms of conjugated path length, with what we have used for PA and PPP. For shorter chains, the conventional MOPAC-FF treatment was employed.

TABLE 2: PM3 Values of α, β, and γ for Terminal Substitution by X/Y at Either End of PA = $-(C_2H_2)_{50}-$ and PPP = $-(C_6H_4)_{26}-$ Chains

PA

	X			
Y	H	NH_2	NO_2	CN
		α (au)		
H	8806.4	8895.6	8777.8	8884.5
NH_2		8977.8	8860.6	9028.6
NO_2			8883.9	9052.2
CN				9085.0
		β (10^3 au)		
H	0	51.066	83.117	49.178
NH_2		0	133.97	96.174
NO_2			0	38.242
CN				0
		γ (10^6 au)		
H	722	733	729	746
NH_2		745	740	749
NO_2			747	754
CN				753

PPP

	X			
Y	H	NH_2	NO_2	CN
		α (au)		
H	3922.7	3985.3	3962.0	3958.8
NH_2		4047.4	4024.0	4047.8
NO_2			4000.3	4024.1
CN				4048.2
		β (10^3 au)		
H	0	6.516	5.849	3.200
NH_2		0	12.57	9.683
NO_2			0	2.598
CN				0
		γ (10^6 au)		
H	38.4	39.6	39.1	39.1
NH_2		40.7	40.7	40.2
NO_2			39.8	39.7
CN				39.7

TABLE 3: PM3 β Values (10^3 au) for Various Substitution Patterns on the Terminal Rings of a PPP Chain Containing 26 Phenyl Rings[a]

X1−Y1 (X2, Y2, Y3 = H)

	X1			
Y1	H	NH_2	NO_2	CN
H	0	1.020	2.887	2.134
NH_2	1.013	0.024	3.873	3.144
NO_2	2.899	3.913	0.204	0.750
CN	2.073	2.707	0.837	0.439

X1−Y2 (X2, Y1, Y3 = H)

	X1			
Y2	H	NH_2	NO_2	CN
H	0	1.020	2.887	2.132
NH_2	7.309	5.458	9.368	8.617
NO_2	5.784	6.823	2.938	3.665
CN	3.168	4.185	0.2693	1.027

X1−Y3 (X2, Y1, Y2 = H)

	X1			
Y3	H	NH_2	NO_2	CN
H	0	1.020	2.887	2.132
NH_2		0	3.911	3.151
NO_2			0	1.027
CN				0

X2−Y2 (X1, Y1, Y3 = H)

	X2			
Y2	H	NH_2	NO_2	CN
H	0	6.516	5.849	3.200
NH_2		0	12.57	9.683
NO_2			0	2.598
CN				0

[a] The location of X1, X2, Y1, Y2, and Y3 is shown in Figure 5.

Our results are shown in Figure 7a−c. As in section III.B, substitution sometimes leads to large values of β but only modest changes in α and γ. The growth of α and γ with *N* is, again, supralinear for short chains and linear for long chains. However, if oscillations are ignored, β now increases linearly with *N* regardless of the chain length.

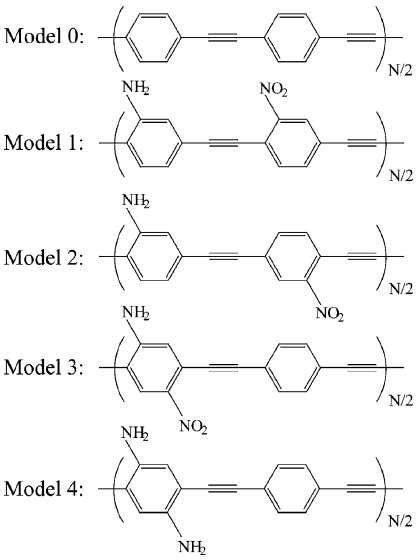

Figure 6. Four models for periodic D/A substitution on phenyl rings of PPE.

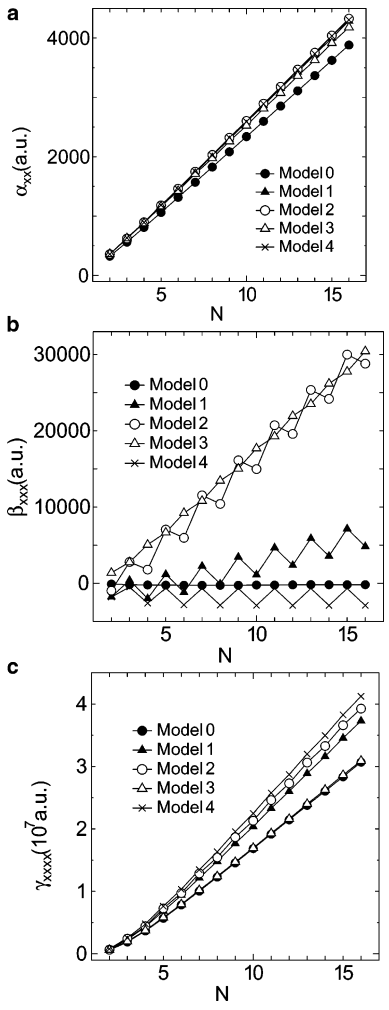

Figure 7. Dependence of (hyper)polarizabilities on the number of phenyl rings, *N*, for various models of periodic D/A substituted PPE: (a) α, (b) β, and (c) γ.

For α, all models yield an increase over the unsubstituted species by about 10%. In the case of γ, model 3 shows essentially no effect whereas the other three models yield an enhancement between 22% and 35%. The largest γ is attained when one phenyl ring is disubstituted with NH_2 groups in the ortho and meta positions (i.e., model 4). By far the largest enhancements of β occur for models 2 and 3. These are the models that contain a donor substituent and an acceptor substituent trans to one another (with respect to the longitudinal axis), either both on the same phenyl ring or one on each phenyl ring of the unit cell.

All substituted chains show a substantial oscillation of β values from *N* even to *N* odd. From the results for models 1 and 2, the deviations from linear behavior are consistent with an increase in β due to donor substitution and a somewhat smaller decrease due to acceptor substitution. Model 3 shows only a weak oscillation because the donor and acceptor are on the same ring and the effects tend to cancel. Finally, in the case of model 4 (which has only donor substituents) the oscillation has a different origin. It arises because of the breakdown of centrosymmetry for even *N* and restoration of that symmetry for odd *N*.

D. Block Copolymer with a Quantum Well Structure. Quantum well electronic and optical devices have matured into commercial products and have the promise of being more useful in the future. As early as 1969, Esaki and Tsu[21,22] found that a heterostructure of alternating semiconductor layers with different band gaps exhibited novel properties. Such quantum well structures have been found to exhibit large optical nonlinearity. Various optical bistable devices,[23] all-optic directional couplers,[24] and degenerate four-wave mixers[25] have been developed, although progress in NLO applications has been fairly slow. A good review of quantum well devices can be found in ref 26.

One advantage of the elongation method, as opposed to a band structure treatment, is that it can readily deal with block copolymers. As an example, we consider here the π-conjugated polyheterol system shown in Figure 8a. Each unit cell contains five all-trans pyrrole rings followed by five all-trans silole rings. In our calculations, the starting cluster consisted of one such unit cell, which contains the same number of rings as the initial PPP cluster. This unit cell was elongated one ring at a time, up to a total of 25 rings.

A local density of states (LDOS) calculation was carried out for the 8th (13th) ring of the 10 (15) ring cluster following the method of ref 14. The 8th ring is located at the center of the first silole block, while the 13th ring is at the center of the second pyrrole block. Our results are displayed in Figure 8b,c where it can be seen that the band gap of the silole block is 5.30 eV as compared to the pyrrole block band gap of 6.55 eV. Although these band gaps are overestimated, the difference between them is reasonable and it is this difference that gives rise to a quantum well.

Our calculated values of α, β, and γ are plotted versus ring number (*M*) in Figure 9a−c, respectively. The (hyper)polarizabilities of pure pyrrole and silole chains are plotted on the same figures for comparison. From Figure 9c, we see that the increment in γ due to adding a pyrrole block is enhanced by a small amount due to copolymerization, while the increment due to the silole blocks decreases more substantially. The same is true of α, but to a lesser extent. For β, copolymerization induces an asymmetry that leads to a roughly constant negative value over each pyrrole block and a roughly constant positive value over each silole block. The magnitude of β in either case is fairly small.

IV. Conclusions

We have applied the elongation-FF method using a semiempirical PM3 Hamiltonian to calculate (hyper)polarizabilities of donor and/or acceptor substituted π-conjugated chains as well

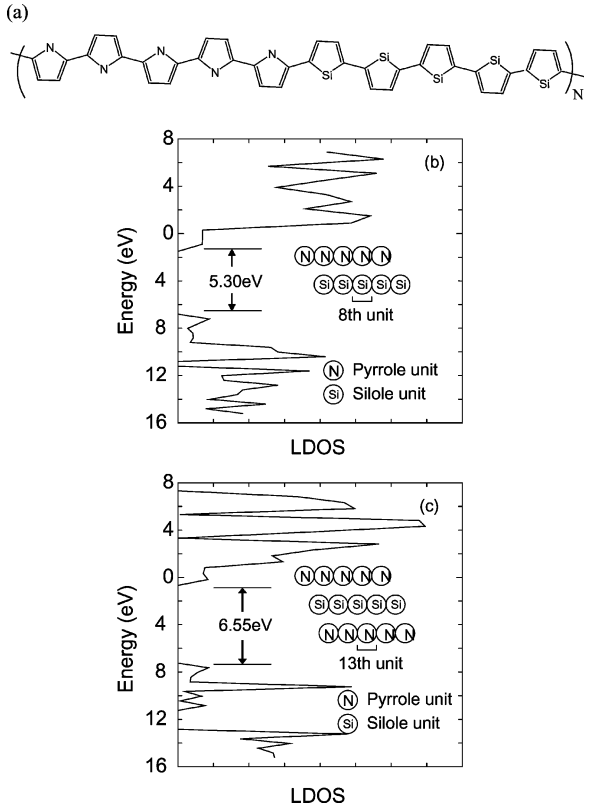

Figure 8. LDOS as a function of energy for the heterol block copolymer chains shown in panel a. The LDOS for the silole unit at the center of the first silole block (starting from the left-hand terminus) is given in panel b for a chain containing 10 units; the LDOS for the pyrrole unit at the center of the second silole block (starting from the left-hand terminus) is given in panel c for a chain containing 15 units.

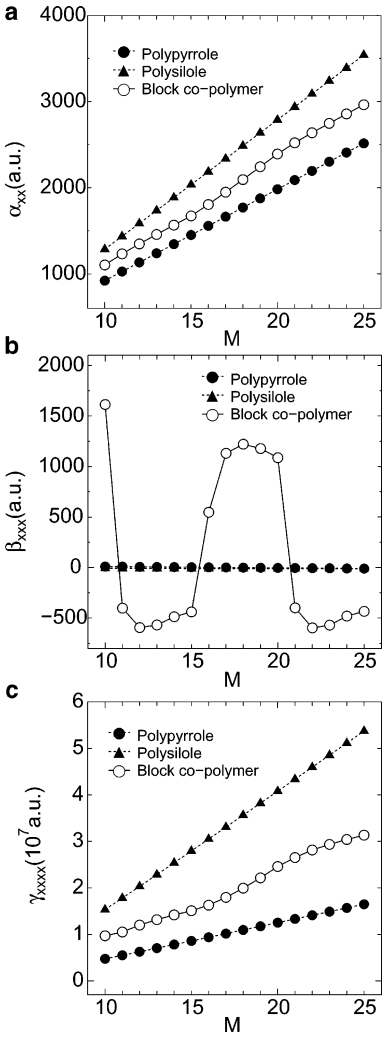

Figure 9. Dependence of α, β, and γ, in panels a−c, respectively, versus the total number of pyrrole plus silole units, *M*, in the block copolymer of Figure 8a.

as a heterol block copolymer. Initial tests on PA chains with a single terminal substituent demonstrate that our method produces reliable results given a starting cluster of sufficient size.

For PA and PPP chains, it was seen that terminal donor/acceptor substituents modify α and γ modestly but that large values of β can be induced. In the latter case, the hyperpolarizability initially grows rapidly with chain length and, then, saturates beyond about 15 −CH═CH− units for PA or 7 phenyl rings for PPP. The largest value at saturation is attained for the NH_2/NO_2 donor/acceptor pair at the ends of a PA chain. The effect of substituents on phenyl rings along the chain backbone was studied for the case of PPE using several different periodic substitution patterns (or models). Although the changes in α and γ are larger than for terminal substitution (of PPP or PA), they remain modest (10−35%) for all models. On the other hand, β increases linearly with *N*, as expected, with the largest slopes being obtained for trans (with respect to the backbone) NH_2/NO_2 substitution either on the same ring of the unit cell or on different rings. There is also an oscillation from *N* even to *N* odd for all models. This oscillation can be rationalized on the basis of the donor versus acceptor strength and, in one case, on the basis of symmetry.

Finally, a heterol block copolymer with a unit cell consisting of 5 consecutive all-trans pyrrole rings followed by 5 consecutive all-trans silole rings was considered. This block copolymer has a quantum well structure since the band gap of the silole blocks is different from that of the pyrrole blocks. The asymmetry due to copolymerization induces a small β that is roughly constant over each block but alternates in sign from one block to the next. The increase in α and γ due to each additional block is enhanced by copolymerization for the pyrrole blocks and diminished more substantially for the silole blocks.

Now that the usefulness of the elongation-FF method has been established, we plan to implement our procedures within an ab initio framework. To reduce the size of the starting cluster and improve the localization, in general, a new density matrix based localization approach is currently under investigation.

Acknowledgment. This work was supported by a Grant-in-Aid for Scientific Research from the Ministry of Education, Culture, Sports, Science, and Technology (MEXT) of Japan and by the Research and Development Applying Advanced Computational Science and Technology of the Japan Science and Technology Agency (ACT-JST). The calculations were performed on the Linux PCs and SGI ORIGIN2000 systems in our laboratory.

References and Notes

(1) Champagne, B.; Kirtman, B. *Handbook of Advanced Electronic and Photonic Materials*; Academic Press: San Diego, 2000; Vol. 9.

(2) Champagne, B.; Jacquemin, D.; André, J. M.; Kirtman, B. *J. Phys. Chem. A* **1997**, *101*, 3158.

(3) Jacquemin, D.; Champagne, B.; Kirtman, B. *J. Chem. Phys.* **1997**, *107*, 5076.

(4) Ladik, J. *Quantum Chemistry of Polymers as Solids*; Plenum: New York, 1987.

(5) André, J. M.; Delhalle, J.; Brédas, J. L. *Quantum Chemistry-Aided Design of Organic Polymers for Molecular Electronics*; World Scientific: London, 1991.

(6) André, J. M.; Mosley, D. H.; Champagne, B.; Delhalle, J.; Fripiat, J. G.; Brédas, J. L.; Vanderveken, D. J.; Vercauteren, D. P. In *Methods and Techniques in Computational Chemistry*: *METECC-94*; Clementi, E., Ed.; STEF: Cagliari, Italy, 1993; Vol. B, Chapter 10, p 423.

(7) Kirtman, B.; Gu, F. L.; Bishop, D. M. *J. Chem. Phys*. **2000**, *113*, 1294.

(8) Bishop, D. M.; Gu, F. L.; Kirtman, B. *J. Chem. Phys*. **2001**, *114*, 7633.

(9) Kirtman, B.; Champagne, B.; Gu, F. L.; Bishop, D. M. *Int. J. Quantum Chem*. **2002**, *90*, 709.

(10) Champagne, B.; Jacquemin, D.; Gu, F. L.; Aoki, Y.; Kirtman, B.; Bishop, D. M. *Chem. Phys. Lett*. **2002**, *373*, 539.

(11) Gu, F. L.; Bishop, D. M.; Kirtman, B. *J. Chem. Phys*. **2001**, *115*, 10548.

(12) Gu, F. L.; Aoki, Y.; Bishop, D. M. *J. Chem. Phys*. **2002**, *117*, 385.

(13) Imamura, A.; Aoki, Y.; Maekawa, K. *J. Chem. Phys*. **1991**, *95*, 5491.

(14) Aoki, Y.; Imamura, A. *J. Chem. Phys*. **1992**, *97*, 8432.

(15) Gu, F. L.; Aoki, Y.; Imamura, A.; Bishop, D. M.; Kirtman, B. *Mol. Phys*. **2003**, *101*, 1487.

(16) Perpète, E. A.; Champagne, B. *J. Mol. Struct.* (*THEOCHEM*) **1999**, *487*, 39.

(17) Frisch, M. J.; Trucks, G. W.; Schlegel, H. B.; Scuseria, G. E.; Robb, M. A.; Cheeseman, J. R.; Zakrzewski, V. G.; Montgomery, J. A., Jr.; Stratmann, R. E.; Burant, J. C.; Dapprich, S.; Millam, J. M.; Daniels, A. D.; Kudin, K. N.; Strain, M. C.; Farkas, O.; Tomasi, J.; Barone, V.; Cossi, M.; Cammi, R.; Mennucci, B.; Pomelli, C.; Adamo, C.; Clifford, S.; Ochterski, J.; Petersson, G. A.; Ayala, P. Y.; Cui, Q.; Morokuma, K.; Malick, D. K.; Rabuck, A. D.; Raghavachari, K.; Foresman, J. B.; Cioslowski, J.; Ortiz, J. V.; Baboul, A. G.; Stefanov, B. B.; Liu, G.; Liashenko, A.; Piskorz, P.; Komaromi, I.; Gomperts, R.; Martin, R. L.; Fox, D. J.; Keith, T.; Al-Laham, M. A.; Peng, C. Y.; Nanayakkara, A.; Gonzalez, C.; Challacombe, M.; Gill, P. M. W.; Johnson, B. G.; Chen, W.; Wong, M. W.; Andres, J. L.; Head-Gordon, M.; Replogle, E. S.; Pople, J. A. *Gaussian 98*; Gaussian, Inc.: Pittsburgh, PA, 1998.

(18) Morley, J. O.; Docherty, V. J.; Pugh, D. *J. Chem. Soc., Perkin Trans. 2* **1987**, 1351.

(19) Matsuzawa, N.; Dixon, D. A. *Int. J. Quantum Chem*. **1992**, *44*, 497.

(20) Jacquemin, D.; Champagne, B.; Perpète, E. A.; Luis, J. M.; Kirtman, B. *J. Phys. Chem. A* **2001**, *105*, 9748.

(21) Esaki, L.; Tsu, R. *IBM Internal Research Report RC 2418*; Mar 26, 1969.

(22) Esaki, L.; Tsu, R. *IBM J. Res. Dev*. **1970**, *14*, 61.

(23) Gibbs, H. M. *Optical Bistability*: *Controlling Light with Light*; Academic Press: New York, 1985.

(24) Miller, D. A. B.; Chemla, D. S.; Eilenberger, D. J.; Smith, P. W.; Gossard, A. C.; Wiegmann, W. *Appl. Phys. Lett*. **1983**, *42*, 925.

(25) Jin, R.; Chuang, C. L.; Gibbs, H. M.; Koch, S. W.; Polky, J. N.; Pubanz, G. A. *Appl. Phys. Lett*. **1988**, *53*, 1791.

(26) Nag, B. R. *Physics of Quantum Well Devices*; Kluwer Academic: Boston, 2000.